Organic Geochemistry 41 (2010) 1312–1325

Contents lists available at ScienceDirect

Organic Geochemistry

journal homepage: www.elsevier.com/locate/orggeochem

Chemometric study of functional groups in Pennsylvanian gymnosperm plant organs (Sydney Coalfield, Canada): Implications for chemotaxonomy and assessment of kerogen formation

José A. D'Angelo [a,b,*], Erwin L. Zodrow [c], Alejandra Camargo [b,d]

[a] Instituto Argentino de Nivología, Glaciología y Ciencias Ambientales (IANIGLA), CCT – CONICET-Mendoza, Avda. Ruiz Leal s/n Parque Gral. San Martín (5500) Mendoza, Argentina
[b] Área de Química, Instituto de Ciencias Básicas, Universidad Nacional de Cuyo, Centro Universitario, M5502JMA Mendoza, Argentina
[c] Palaeobotanical Laboratory, Cape Breton University, Sydney, Nova Scotia, Canada B1P 6L2
[d] Laboratorio de Análisis de Residuos Tóxicos, Facultad de Ciencia Agrarias, Universidad Nacional de Cuyo, Alte. Brown 500, Chacras de Coria, 5505 Mendoza, Argentina

ARTICLE INFO

Article history:
Received 28 May 2010
Received in revised form 9 September 2010
Accepted 23 September 2010
Available online 26 September 2010

ABSTRACT

The samples comprise the foliage of four pteridosperm-medullosalean plant fossil species of differing preservation states and one of a cordaitean species from two Canadian Maritime sub-basins of Carboniferous age (300 Ma; Sydney and Stellarton coalfields, Nova Scotia, respectively). Included in the sample set were some coal samples from Sydney Coalfield, along with published data for coal macerals for comparison. By applying Schulze's maceration process to the fossil foliage to obtain the cuticles, five sample forms evolved, viz. compressions, cuticles and fossilized cuticles, and acidic and alkaline solutions from Schulze's process, to which was added the Sydney coal samples as the sixth form. Area integration of the absorbance spectra from solid and liquid state Fourier transform infrared (FTIR) spectroscopy, produced functional chemical parameters which were organized into a data matrix of eight variables and 62 samples (8×62 matrix). Since we were interested in grouping the sample forms as a function of phytochemistry (functional groups) to assess primarily the palaeophytotaxonomic potential as a general approach to Carboniferous taxonomy, principal components were extracted from the matrix, and a subset of 4×33 samples in order to refine the grouping results from the initial component analysis. In each case, a two component model resulted, accounting for least 80% of the cumulative variance.

Overall, the results are encouraging in offering increasing support for fossil-leaf chemotaxonomy, but bearing in mind the limited sampling number (56) and restricted sampling of genera (5). Apart from this general conclusion, which supports our previous FTIR work vis-à-vis chemotaxonomy, we noted functional-group similarities in our FTIR data with types of kerogen and coal macerals. On this basis, we hypothesize that, in combination with the different preservation states of our fossil specimens, these factors have a bearing on kerogen genesis from plant material, i.e. the oil and gas prone Types I and II.

© 2010 Elsevier Ltd. All rights reserved.

1. Introduction

Abundant types of Pennsylvanian-age fossil organs of North America are fragments of gymnosperm foliage and, to a lesser extent, detached ovules of seed ferns. Their taxonomy is largely based on morphology, augmented by the morphology of cuticles (see Cleal and Zodrow, 1989). Lately, attempts have been initiated to also use the cuticles of seed ferns and ferns in continued studies of the distribution and contents of functional groups using Fourier transform infrared (FTIR) spectroscopy methods (summarized by Zodrow et al., 2009), noting also in this respect the use of pyrolysis gas chromatography coupled with mass spectrometry (py-GC/MS) (Lyons et al., 1995; Zodrow and Mastalerz, 2001, 2002). The overall aim of these studies has been, and continues to be, enlargement of the number of taxonomic classification parameters for Carboniferous gymnosperms by complementing the known morphologically-derived taxonomic criteria with phytochemical parameters derived from modern spectrochemical methods. Results are basic to development of more natural species for a more natural phylogeny that eventually will replace the existing one (see Taylor and Taylor, 1993).

The present study is not only based on comparatively larger sample sizes involving five gymnosperm species, not all of the same preservation type, but also on a new sampling methodology comprising six sampling forms, i.e. compressions, cuticles, fossilized cuticles, acidic and alkaline solutions from Schulze's maceration process which extracts cuticles from the compressions, and associated coal samples as a sixth form (see Zodrow et al., 2009). Data obtained from the FTIR analyses were statistically evaluated

* Corresponding author. Fax: +54 261 5244201.
E-mail address: joseadangelo@yahoo.com (J.A. D'Angelo).

0146-6380/$ - see front matter © 2010 Elsevier Ltd. All rights reserved.
doi:10.1016/j.orggeochem.2010.09.010

by way of principal components methods for the purpose of isolating grouping of sample forms as a function of the functional groups to evaluate more rigorously the potential for palaeophytochemotaxonomy of Carboniferous plant fossils. Based on similarity amongst plant fossils, coal, and kerogen types, the formation of kerogen from plant life is assessed.

2. Material

2.1. Provenance and sample forms

The fossil plant samples are from the Carboniferous Sydney and Stellarton Sub-basins, Nova Scotia, Canada, where the Sydney Coalfield is the younger of the two (Fig. 1). The Sydney samples (Fig. 2A–E) originate from the gray, silty shale roof rocks of two coal seams (Fig. 3) near the Asturian–Cantabrian floral boundary (Dimitrova et al., in press) from which coal samples (vitrain) were also collected. The Stellarton samples (Fig. 2F) were collected from the arenaceous roof rocks of the 13 m thick Foord Seam (Fig. 4).

"Fossils as preserved" and "fossils derived" represent the two categories used for the six sample forms (Table 1). The first refers to plant fossils dug from the roof rocks, which generally required HF treatment to free the compression (synonym adpression; Shute and Cleal, 1987) or fossilized cuticle. Coal samples were not chemically treated. The second category comprises the cuticle and, as a result of Schulze's process, the acidic and alkaline solutions. Table 2 summarizes the fossil and FTIR sample information and cites the nomenclature for each species (omitted from the text for brevity)

3. Methods

3.1. Schulze's maceration (oxidation)

The cuticle was obtained by way of Schulze's (1855) process, whereby the compression is treated with a maceration solution (4–6 g $KClO_3$ in 150 ml non-fuming HNO_3), followed by an alkaline solution of 4.5% NH_4OH (see Cleal and Zodrow, 1989). Macerating time was variable from 24 h to >200 h, i.e. until the alkaline treatment (10 min) showed no further reaction. The extracted cuticle was rinsed and washed in distilled water for at least one and a half days. Of the retained acidic and alkaline solutions (Table 2), the latter was by far the most informative as it accumulated most of the hydrocarbon net weight loss from the compressions (see Zodrow et al., 2009, Figs. 6 and 7). Table 3 summarizes the net weight loss from two compression species as a result of Schulze's process.

3.2. Liquid and solid state FTIR spectra

A Nicolet Thermo-Electron 6700 spectrometer, equipped with attenuated total reflectance (ATR) capability (Smith, 1996) and DTGS-CsI detector, was used to analyze the acidic and alkaline solutions. However, the highly corrosive nature of the acidic solution damaged the ATR set-up, and only one experiment was carried out using *Alethopteris pseudograndinioides*.

Compressions, fossilized cuticles, cuticles and coal were analyzed using KBr pellets (0.5–2.0 mg sample with 250 mg KBr and compressing the ground mixture into a pellet). In all cases, 256 scans per sample were collected at a resolution of 4.0 cm^{-1}, over 4000–500 cm^{-1}.

3.3. Qualitative and semi-quantitative FTIR analyses

Table 4 summarizes definitions of the area ratios, together with band regions involved for calculation and interpretation. Band assignments for functional groups were made according to Painter et al. (1981a,b, 1985), Colthup et al. (1990), Shurvell (2002), Stuart (2004) and Wang and Griffiths (1985). Different treatments of digitized spectra were applied to refine and improve the information provided by FTIR spectroscopy. The following techniques were employed: area integration methods (e.g. Sobkowiak and Painter, 1992; D'Angelo, 2004; D'Angelo and Marchevsky, 2004), and calculation of area ratios (e.g. Mastalerz and Bustin, 1993; D'Angelo, 2006; Zodrow et al., 2009). A Fourier self-deconvolution procedure (Kauppinen et al., 1981a,b), specifically used to separate the

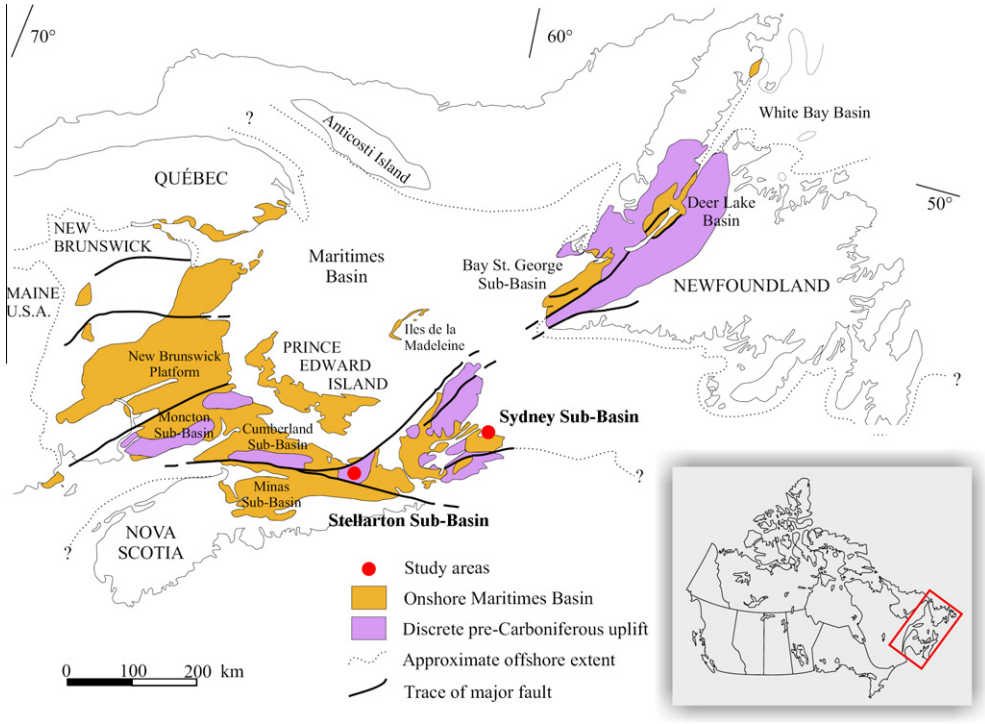

Fig. 1. Locations of the Carboniferous Sydney and Stellarton Sub-Basins, Nova Scotia, within the geologic setting of the Canadian onshore Maritimes Basin.

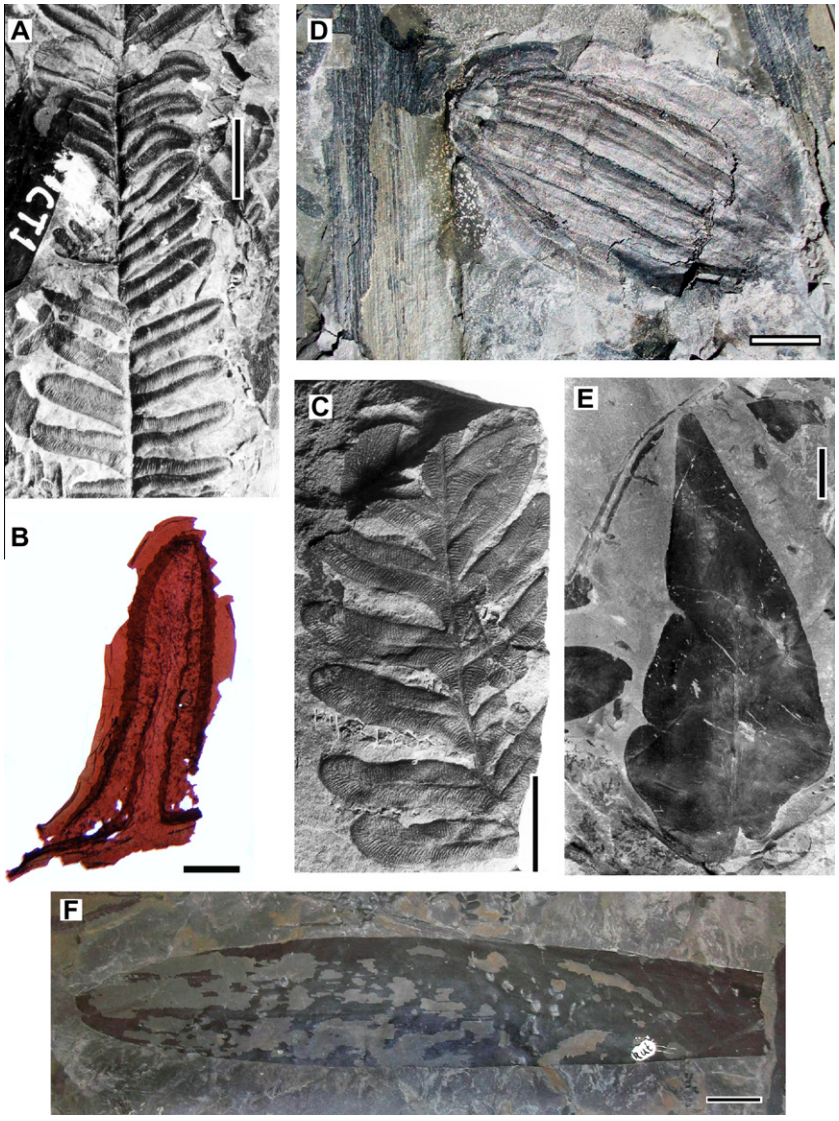

Fig. 2. Hand specimens from Sydney (A–E) and Stellarton Sub-Basins (F). (A) Compression; *Alethopteris ambigua*. CT1 = studied cuticle. Scale bar = 1 cm. (B) Fossilized cuticle, *Alethopteris ambigua;* scale bar 1 mm. (C) Compression, *Alethopteris pseudograndinioides*; scale bar 1 cm. (D) Compression, *Trigonocarpus grandis*; scale bar 1 cm. (E) Compression, *Macroneuropteris scheuchzeri*; scale bar 1 cm. (F) Compression, *Cordaites principalis*; scale bar 2 cm.

aliphatic C—H stretching region (ca. 3000–2825 cm^{-1}), and a resolution enhancement procedure were also employed.

Spectral resolution enhancement is a method for increasing the apparent resolution of overlapping bands in order to more easily determine the number of bands and their wavelengths. The method is based on subtracting a multiple of the second derivative from the original spectrum (Rosenfeld and Kak, 1982; Almendros and Sanz, 1992). Different multiples of the second derivatives were employed according to the type of sample: 100× (cuticle), 200× (fossilized cuticle) and 220× (compression and coal).

3.4. Strategy for principal component analysis (PCA) of FTIR-derived data: a multivariate approach

PCA is a nonparametric, pattern-recognizing method that can be used at its most basic for visualizing multivariate data in a straightforward and simplified fashion. This is accomplished through data reduction, where the number of components is less than the number of variables, in line with preference for parsimonious scientific explanation, or Ockham's Razor, and through groupings using component scores (e.g. Jolliffe, 2002; Lattin et al., 2002; Rencher, 2002; Anderson, 2003; Johnson and Wichern, 2008; Izenman, 2008). We decided to retain the number of components whose cumulative variance was close to 90% (see Kaiser, 1960 for other methods; Kendall, 1965). Inherent assumptions include orthogonal (uncorrelated) components, no error variance and data structure. Our strategy was to evolve a set of data groupings to evaluate it as a function of chemical structure (functional groups). PCA was performed using the computer program STATISTICA® (StatSoft Inc., 2001) on raw data consisting of eight variables with 62 determinations each.

4. Results and discussion

4.1. Qualitative chemical characterization

Only representative FTIR spectra of the different sample forms are shown in Figs. 5 and 6. Irrespective of the six sample forms, FTIR spectra therefrom exhibit common characteristics (functional groups), summarized as follows. A broad and intense band centered between 3400 and 3300 cm^{-1} is generally attributed to H-bonded hydroxyl (OH) stretch (Fig. 5A) in alcohols and phenols.

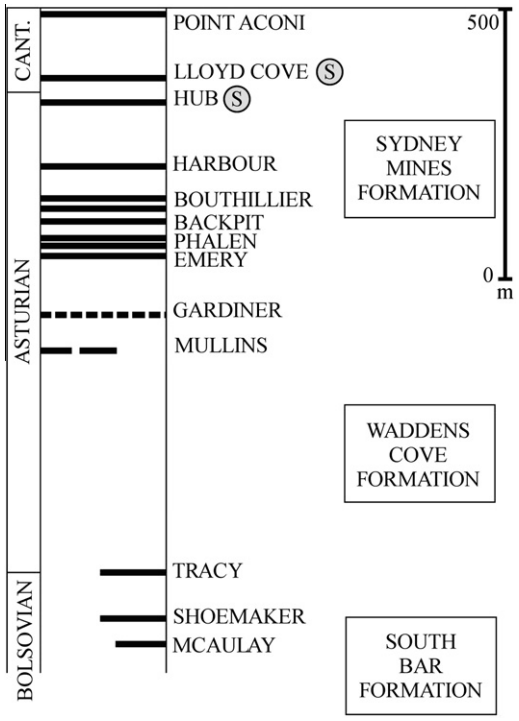

Fig. 3. Onshore coal stratigraphy, Sydney Sub-Basin. Sampled roof rocks of coal seams (S). Lloyd Cove Seam: fossilized cuticles of *Alethopteris ambigua*, compressions of *A. pseudograndinioides* and *Trigonocarpus grandis*. Hub Seam: compressions of *A. ambigua* and *Macroneuropteris scheuchzeri*. Coal (vitrain) samples come from the top parts of the Lloyd Cove and Hub Seams.

Additional bands having the same assignment occur only for the acidic (at 3360 cm^{-1}) and alkaline solutions (at 3190 cm^{-1}; Fig. 5B and C, respectively). A band centered at ca. 3050 or 3040 cm^{-1} (absent from most of the cuticles and acidic solution) was assigned to aromatic C—H stretching vibrations.

All the sample forms exhibited distinct peaks in the 3000–2800 cm^{-1} region which, based on group frequency tables from the literature (Colthup et al., 1990; Shurvell, 2002 and Stuart, 2004), were ascribed to aliphatic C—H stretching. These were assigned to antisymmetric methylene (CH_2) stretch (2936–2916 cm^{-1}) and symmetric CH_2 stretch (2863–2843 cm^{-1}).

The region below 2000 cm^{-1} exhibited differences depending on the kind of sample, and of particular interest was the region 1800–1480 cm^{-1}. Peaks of different intensities assigned to stretching of carboxyl (COOH) and other carbonyl (C=O) groups (e.g. singly conjugated ketones) occurred in the 1740–1700 cm^{-1} region. Cuticles and fossilized cuticles showed a medium to high intensity C=O peak, with maximum absorption in the 1720–1712 cm^{-1} range (Figs. 5D and 6A and B), which was assigned to aromatic carbonyl groups.

The acid solution spectrum (Fig. 5B) showed other peaks belonging to the inorganic matrix. Thus, NO_3^- from the HNO_3 used absorbed strongly and broadly near 1400 cm^{-1}; S=O stretching in alkyl and aryl sulfoxides gave rise to strong absorption at 1040 cm^{-1} and the peak at 1320 cm^{-1} could be assigned to the antisymmetric stretch of SO_2 groups (Colthup et al., 1990). Pyrite, known to be associated with compressions, is likely the sulfur source (Zodrow and Mastalerz, 2009; Fig. 11).

Spectra from the alkaline solution (Fig. 5C) showed the following typical peaks: NH_2 scissor deformation at 1650–1590 cm^{-1} (this group absorbs near 1600 cm^{-1}), NH_3^+ absorption near 1600–1520 cm^{-1}, NH_4^+ vibration at 1400 cm^{-1} and NH_2 in plane rocking at 1105 cm^{-1} (Colthup et al., 1990; Shurvell, 2002; Stuart, 2004).

For all the sample forms, aliphatic (alkyl) C—H deformations were represented by medium intensity peaks at 1460 cm^{-1}, 1457 cm^{-1} and 1436 cm^{-1} (Figs. 5 and 6) (assigned to either CH_3 antisymmetric or CH_2 scissor deformation) and a medium intensity peak centered at 1384 cm^{-1} [CH_3 umbrella deformation; see

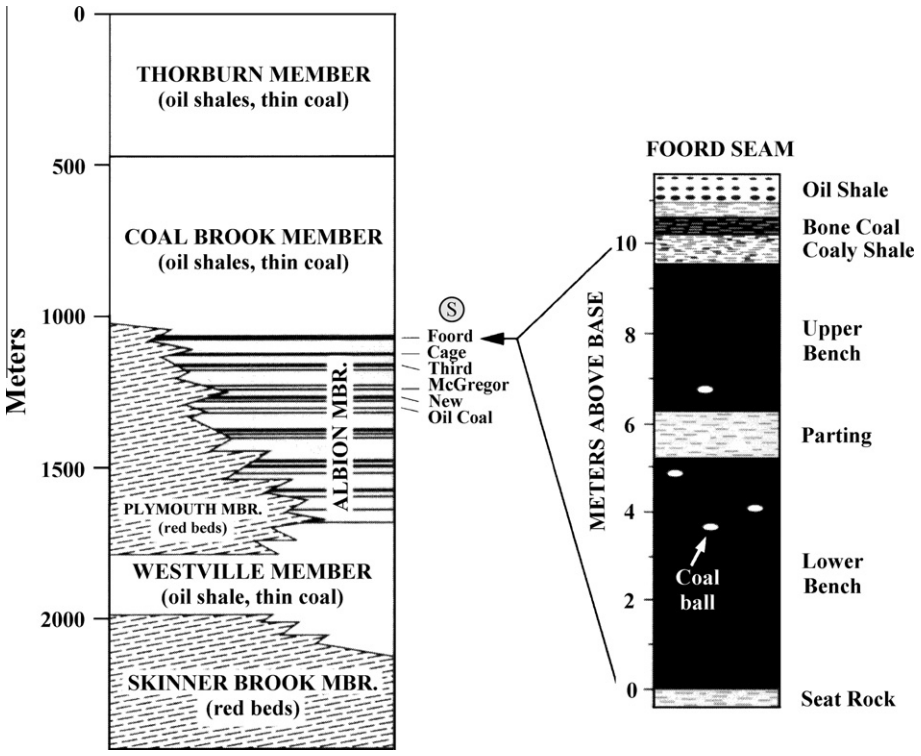

Fig. 4. Coal stratigraphy and sampled roof rocks from the Foord Seam (S), Stellarton Sub-Basin: *Cordaites principalis*. Source Lyons et al. (1997).

Table 1
Sample forms used.

Form	Description
Fossil preserved in rock	
Compression	Conceptualized by an analogue model of the anatomy of an extant leaf: "vitrinite (mesophyll) + cuticle (biomacropolymer) = compression" (Zodrow et al., 2009)
Fossilized cuticle	Cuticle, where coalified layer (vitrinite) is no longer preserved, only the cuticle itself (summarized by Zodrow and Mastalerz, 2009)
Vitrain	Bright and shiny banded bituminous coal
Derived from Schulze's process	
Cuticle	Thin film of biomacropolymeric structure obtained from compression
Acid and alkaline solutions	From extraction of cuticle, containing organic matter macerated from the compression

Table 2
Taxonomy and fossil and FTIR-sample information. Sydney Coalfield, Nova Scotia, Canada (n.a., not available).

Taxonomy/morphospecies	Fossil-sample			Liquid/solid-state FTIR sample		
	Sample description pinules/size	Preservation state	No. pinnules analyzed	Ml of acid/alkaline solution (no. of samples)	Sample form[a]	Single cuticles[b] mg (no. of samples)
Pteridosperms (gymnosperm)						
Alethopteris pseudograndinioides (Zodrow and Cleal, 1998)	Entire pinnule, no rachis	Compression	200	Acid 60 (1)	Acid	n.a.
				Alkaline 80 (1)	Alkaline	n.a.
					Cuticle	1.5 (5)
					Compression	1.7 (6)
A. ambigua (Lesquereux) *pars* (Zodrow and Cleal, 1998)	Entire pinnule, no rachis	Compression	400	Alkaline 80 (1)	Alkaline	n.a.
					Compression	1.7 (6)
					Cuticle	1.6 (6)
	Entire pinnule, no rachis	Fossilized cuticle	80		Fossilized Cuticle	1.8 (2)
Trigonocarpus grandis Lesquereux) (Cleal and Zodrow, 2010)	8 cm × 4.5 cm sized ovule	Compression	Entire ovule	Alkaline 30 (1)	Alkaline	n.a.
					Cuticle	1.8 (3)
					Compression	1.9 (5)
Macroneuropteris scheuchzeri (Hoffmann) (Cleal et al., 1990)	Entire and fragmentary	Compression	30	Alkaline 25 (1)	Alkaline	n.a.
	Pinnules, no rachis				Cuticle	1.6 (1)
					Compression	1.7 (6)
Gymnosperm						
Cordaites principalis (Germar) Zodrow et al., 2000b	30 cm × 6.5 cm	Compression	Entire	Alkaline 45 (1)	Alkaline	n.a.
	Fragmentary leaf		Fragment		Cuticle	1.9 (4)
					Compression	1.4 (4)
Total number of samples				(6)		(48)

[a] Compression (see Table 1).
[b] Average, where a cuticle of a pteridosperm pinnule may reach 2 mg and coalified compression 3 mg (on a dry basis).

Gauglitz and Vo-Dinh (2003) for definitions of CH_2 and CH_3 group vibrations]. However, a contribution of some silicate mineral impurities should not be ruled out. The broad band at 1275 cm^{-1} likely indicates the presence of aromatic units derived from lignin (methoxyphenols; Durig et al., 1988; Zodrow et al., 2000a).

Some low intensity bands occurred in the 900–700 cm^{-1} region. Compressions, fossilized cuticles, alkaline and acidic solutions, and the coal samples showed bands at 866 cm^{-1}, 825 cm^{-1}, 752 cm^{-1}, 736 cm^{-1} and 700 cm^{-1}, assigned to aromatic C—H out-of-plane bending (e.g. Fig. 5A–C). Cuticles obtained using Schulze's process rarely showed aromatic bands in this region. Instead, there was a band at 850 cm^{-1} that could tentatively be assigned to CH_2 vibrational modes (Fig. 5D; cf. Fig. 8C of Zodrow and Mastalerz, 2001). We therefore conclude that the aromatic and aliphatic functional groups for the alkaline and acidic solutions from macerating the compression could only have originated from the vitrinite component (or some other maceral) which was likely the remains of the cellulose-based mesophyll of the leaves (Lyons et al., 1992) and not those from the biomacropolymeric cuticle (Zodrow and Mastalerz, 2007, Fig. 12).

4.1.1. Resolution-enhanced spectral bands

The 1900–1460 cm^{-1} region (delimited in Fig. 6), more than any other, was of particular interest to the study of carbonyl groups and other oxygen- and nitrogen-containing structures. These groups play an important role in determining some of the structural changes related to organic matter (OM) transformation. In turn, the information may relate to organic precursors of kerogen and to preservation processes (e.g. oxidation of OM and formation of fossilized cuticles).

Resolution enhancement is a digital processing technique used in this study to reveal absorption peaks where only shoulders were evident in the original spectra. It should be noted that the application of more complex signal processing techniques (e.g. peak deconvolution) was beyond the scope of the study. Since most of the sample forms (exceptions are alkaline and acidic solutions) showed similar features after resolution enhancement, only *A. ambigua* fossil forms and one coal sample were selected for data presentation. In Fig. 7A–D the originals are superimposed on the resolution-enhanced spectra (bottom spectrum of A–D). Spectra from cuticles and fossilized cuticles

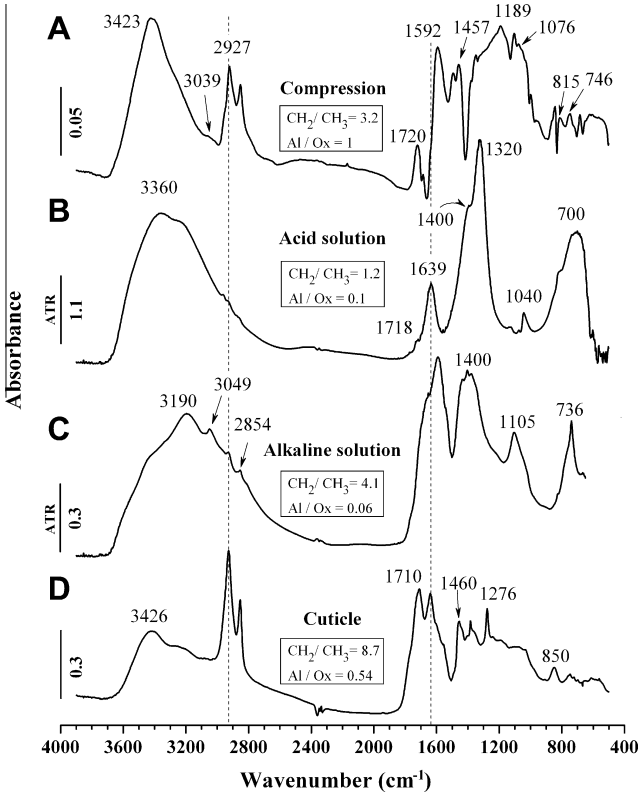

Fig. 5. FTIR spectra of *Alethopteris pseudograndinioides*. Sample forms showing different spectral stages during application of Schulze's process to extract the cuticle. (A) Compression prior to maceration. (B) Acidic and (C) Alkaline solutions. (D) Extracted cuticle (ATR, attenuated total reflection).

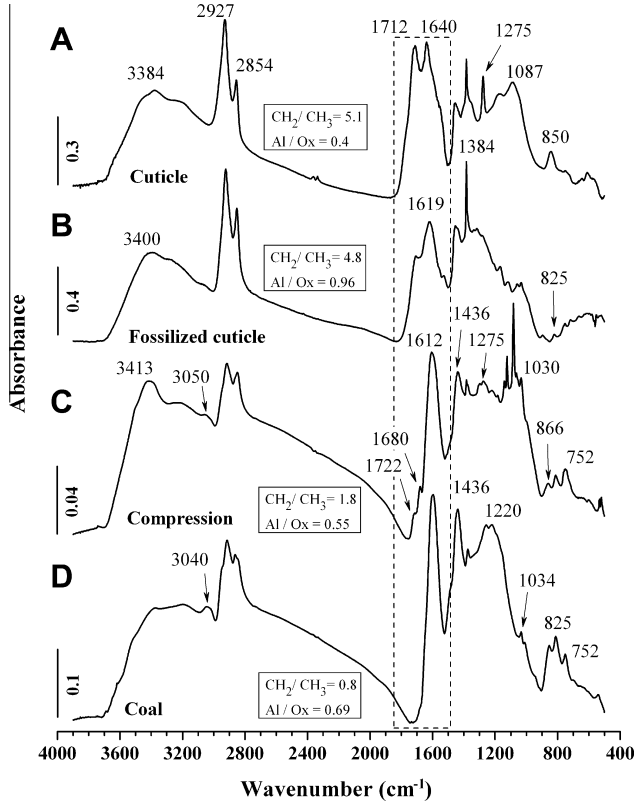

Fig. 6. Comparison of FTIR spectra of *Alethopteris ambigua*: (A) cuticle obtained by Schulze's process. (B) Fossilized cuticle. (C) Compression. (D) Coal. Details of the delimited zone are shown in Fig. 7.

(Fig. 7A and B, lower spectra) showed differentiation of C=O groups. A peak at 1724 cm^{-1} could be assigned to aromatic carbonyl groups and the neighboring shoulder at 1766 cm^{-1} might be due to normal aliphatic ester carbonyl groups, and other oxygen-containing groups, such as cyclic esters or heterocyclic structures (Almendros et al., 1999). In contrast, the compression spectrum showed only aromatic carbonyl groups (at 1722 cm^{-1}; Fig. 7C, lower spectrum). Noted was a decrease in carbonyl peak intensity from cuticles to fossilized cuticles and to compressions, and carbonyl absorption was virtually absent from the coal samples, as confirmed by the resolution-enhanced spectrum (Fig. 7D). All the sample forms showed a broad, intense and non-specific band with maximum absorption in the range 1640–1608 cm^{-1}, produced by a contribution (overlapping bands) from several groups. These include aromatic, oxygen- and nitrogen-containing structures, including conjugated carboxyl and amide groups (1680, 1660, 1650 cm^{-1}) as shown by resolution-enhanced spectra (Fig. 7A–D, lower spectra). Furthermore, the additional peak maximizing in the range 1556–1535 cm^{-1}, traditionally assigned to amide functionality, was also noted (particularly evident in fossilized cuticles, Fig. 7B, lower spectrum). Compression samples showed a peak at 1511 cm^{-1} (Fig. 7C, lower spectrum) assigned to aromatic or unsaturated structures.

4.2. Semi-quantitative comparison with coal macerals and kerogen types

In this section some semi-quantitative data (Table 5) are used to investigate maturity and similarities with coal macerals and kerogen types in an attempt to characterize the differences in functional group chemistry within the sample forms. Thus, semi-quantitative IR data from all the forms were compared with some IR data from coal macerals. The comparisons were limited by the availability of published semi-quantitative FTIR data. Some IR data for liptinite and vitrinite (Mastalerz and Bustin, 1996; Guo and Bustin, 1998) with approximately the same rank (vitrinite reflectance, $R_{0\ max}$ 0.52–0.95%) were compared with our IR data. All the sample forms are shown in a diagram of 'A' vs. 'C' factors (as defined by Ganz and Kalkreuth, 1987), similar to the traditional van Krevelen H/C–O/C plot (Fig. 8), indicating similarities with different types of kerogen. Band areas (not peak intensities) were used to calculate 'A' and 'C' factors. The 'A' factor is defined as (3000–2800)/[(3000–2800) + (1650–1520)] and represents changes in the relative intensities of the aliphatic groups. The 'C' factor is defined as (1800–1600)/[(1800–1600) + (1650–1520)], representing changes in the C=O groups (see Table 4). A simplified plot of Fig. 8, indicating the approximate regions of different sample forms studied, is shown in Fig. 9 where ellipses around the groups are used for clarity only.

A more comprehensive evaluation through PCA of the complete set of semi-quantitative FTIR data (Table 5) is given in Section 4.3.

The following results were obtained by utilizing 'A' and 'C' factors (Ganz and Kalkreuth, 1987) and CH_2/CH_3 ratio values.

4.2.1. Acidic solution

The acidic solution from the *A. pseudograndinioides* preparation exhibited the lowest values for aliphatic compounds and CH_2/CH_3 ratio (Table 5), the latter possibly indicating the shortest or most branched aliphatic side chains. The low content of aliphatic and oxygen-containing compounds showed similarities to some vitrinite samples (Fig. 8). It should be mentioned that the alkaline solution of *A. ambigua* exhibited some similarities to the acidic solution of *A. pseudograndinioides*, thereby showing a similar composition to Type III kerogen (Fig. 8).

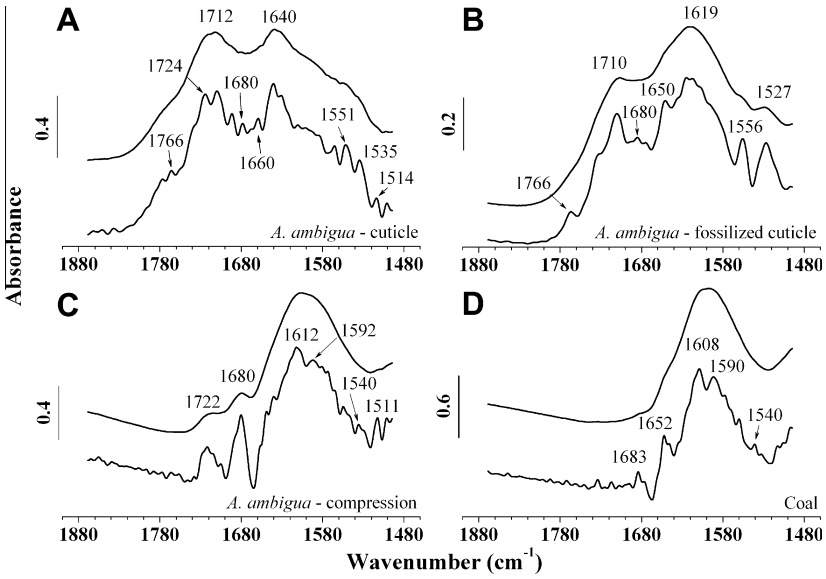

Fig. 7. Detail of 1900–1460 cm^{-1} zone of Fig. 6. The originals are superimposed on the resolution-enhanced spectra (bottom spectrum of A–D). Multiples of the second derivatives employed are 100× (cuticle), 200× (fossilized cuticle), 220× (compression and coal).

Table 3
Net mass loss (%) of compressions resulting from Schulze's process (Sydney Coalfield, Canada).[a]

Morphospecies	Wt. (g)		Ratio (%)	Loss (%)
	Comp.[b]	Cuticle	Cuticle/comp.	
Alethopteris pseudograndinioides	0.2904	0.0430	14.8	85.2
Cordaites principalis	0.0387	0.0070	18.1	81.9

[a] Assuming zero weight loss from the cuticle, loss due to solvent transfer is minimal, as judged from observation under the microscope; cuticles were air-dried at ca. 30 °C.
[b] Compression.

A low CH_2/CH_3 value suggests enhanced carbon–carbon bond breaking of the coalified material during sample oxidation by way of Schulze's process, resulting in comparatively shorter aliphatic chains.

4.2.2. Alkaline solutions

The alkaline solutions showed (Fig. 8) intermediate values for the 'A' and 'C' factors, implying medium to low relative values for both aliphatic and oxygen-containing compounds (mainly C=O compounds). The alkaline solution of *A. pseudograndinioides* was similar in composition to some vitrinite macerals (from medium volatile bituminous coals), whereas *Trigonocarpus grandis* and *Macroneuropteris scheuchzeri* alkaline solutions were chemically similar to some cutinites. The location of the *Cordaites principalis* alkaline solution in the 'A' vs. 'C' factors plot indicated a composition more similar to compression specimens of the different taxa and coal samples.

Table 5 shows that all the alkaline solutions had similar CH_2/CH_3 values (2.9–4.1). Comparison with other sample forms (e.g. compressions and coal macerals) showed medium to low values of the ratio for alkaline solutions. This implies comparatively

Table 4
Definition of semi-quantitative ratios derived from FTIR spectra and interpretation.

Ratio	Band region (cm^{-1}) Band-region ratios	Interpretation and remarks
CH_2/CH_3	3000–2800	Methylene/methyl ratio. Relates to aliphatic chain length and degree of branching of aliphatic side groups (side chains attached to macromolecular structure; Lin and Ritz, 1993a,b). Interpretation: larger value implies comparatively longer and straight chains, smaller value shorter and more branched chains
Al/Ox	(3000–2800)/(1800–1600)	Aliphatic/oxygen-containing compounds ratio. Relative contribution of aliphatic C—H stretching bands (**Al**) to combined contribution of oxygen-containing groups and aromatic carbon (Ox). Interpretation: from higher values decreasing oxygen-containing groups can be inferred, or the lower Al/Ox, the higher Ox
Al/C=C	(3000–2800)/(1600–1500)	Aliphatic/aromatic carbon groups ratio. Relative contribution of aliphatic C—H stretching bands to aromatic carbon groups (C=C). Interpretation: higher values indicate increasing aliphatic groups to aromatic carbon groups. The ratio is equivalent to the **I1** index of Guo and Bustin (1998)
C=O/C=C	(17,000–1600)/(1600–1500)	Carbonyl/aromatic carbon groups ratio. Relative contribution of carbonyl/carboxyl groups (C=O) to aromatic carbon groups. Interpretation: higher values indicate increasing carbonyl/carboxyl groups to aromatic carbon groups
C=O cont	(~1714)/(1800–1600)	Carbonyl contribution. Relative contribution of carbonyl/carboxyl groups (C=O, peak centered near 1714 cm^{-1}) to combined contribution of oxygen-containing groups and aromatic carbon (C=C) structures
C=C cont	(~1600)/(1800–1600)	Aromatic carbon contribution. Relative contribution of aromatic carbon groups (C=C, peak in the region 1650–1520 cm^{-1}, centered near 1600 cm^{-1}) to combined contribution of oxygen-containing groups and aromatic carbon (C=C) structures
'A' factor = Al/(Al + C = C)	(3000–2800)/[(3000–2800) + (1650–1520)]	Relative contribution of aliphatic C—H stretching bands to summation of aliphatic C—H stretching and aromatic carbon structures. Interpretation: according to Ganz and Kalkreuth (1987) it represents changes in the relative intensity of the aliphatic groups
'C' factor = Ox/(Ox + C=C)	(1800–1600)/[(1800–1600) + (1650–1520)]	Relative contribution of oxygen-containing compounds to summation of oxygen-containing structures and aromatic carbon bands. Interpretation: according to Ganz and Kalkreuth (1987) it represents changes in carbonyl/carboxyl groups

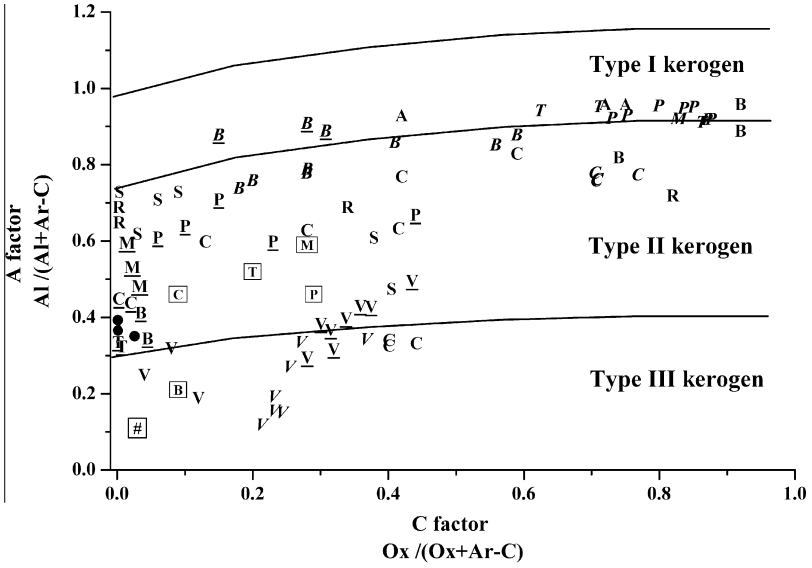

Legend

Coal macerals (literature)

- **S** Sporinite
- **C** Cutinite
- **R** Resinite
- **B** Bituminite
- **A** Alginite
- **V** Vitrinite
- **V** Vitrinite - Medium volatile bituminous coal
- ***V*** Vitrinite - High volatile bituminous coal

Samples (this study)

- ● Coal (vitrain)
- [#] *A. pseudograndinioides* - Acid solution
- [P] *A. pseudograndinioides* - Alkaline solution
- **P** *A. pseudograndinioides* - Compression
- ***P*** *A. pseudograndinioides* - Cuticle
- [B] *A. ambigua* - Alkaline solution
- **B** *A. ambigua* - Compression
- ***B*** *A. ambigua* - Fossilized cuticle
- ***B*** *A. ambigua* - Cuticle
- [C] *C. principalis* - Alkaline solution
- **C** *C. principalis* - Compression
- ***C*** *C. principalis* - Cuticle
- [T] *T. grandis* - Alkaline solution
- **T** *T. grandis* - Compression
- ***T*** *T. grandis* - Cuticle
- [M] *M. scheuchzeri* - Alkaline solution
- **M** *M. scheuchzeri* - Compression
- ***M*** *M. scheuchzeri* - Cuticle

Fig. 8. Kerogen-type diagram of some coal macerals according to variables obtained from infrared spectra, and of the sample forms. Sources: Mastalerz and Bustin (1996; cutinite, vitrinite of medium volatile bituminous coals and vitrinite of high volatile bituminous coals), and Guo and Bustin (1998; cutinite, resinite, bituminite, alginite and vitrinite).

shorter or more-branched aliphatic side chains in alkaline solutions. All the alkaline solutions exhibited a composition similar to Type II kerogen, with the exception of *A. ambigua* (Table 5), which had an intermediate position between compressions and the vitrinite coal macerals (Figs. 8 and 9).

4.2.3. Cuticles

The cuticles obtained from Schulze's process for all the taxa were characterized by high values of both 'A' and 'C' factors, indicating high contents of aliphatic and oxygen-containing compounds, respectively. The results indicate a composition similar to some coal macerals, viz. alginite, bituminite and cutinite (Fig. 8). The exception was the relatively lower value for the 'C' factor for some samples of *A. ambigua* (Table 5 and Fig. 8). The lowest CH_2/CH_3 values were recorded for *C. principalis* and *M. scheuchzeri* (ca. 1.1) whereas medium values were obtained for *A. ambigua* (3.8–5.1), implying comparatively shorter and more-branched aliphatic structures (one exception was the cuticle from the axis of one specimen of *A. ambigua* showing a notably higher value). Distinctly high CH_2/CH_3 values (>10, Table 5) were obtained for cuticles of the three ovules of *T. grandis* found in physical association with foliage of *A. pseudograndinioides.* These results suggest that *A. pseudograndinioides*, and especially *T. grandis*, contain long and unbranched aliphatic structures. More generally, cuticle samples of all the taxa were located (approximately) at the boundary between kerogen Types I and II (Figs. 8 and 9).

4.2.4. Fossilized cuticles

The fossilized cuticles of *A. ambigua* had a composition similar to Type I kerogen, as evident from the medium to high values of the 'A' and of 'C' factors, thereby revealing medium to high contributions from aliphatic and oxygen-containing compounds, respectively. These factors and the CH_2/CH_3 value were similar to those for cuticles (obtained from Schulze's process) for *A. ambigua* (Table 5, Figs. 8 and 9).

4.2.5. Compressions

These were similar in composition to some resinite, sporinite and some vitrinite coal macerals, and to the coal samples (Fig. 8), but those of *A. pseudograndinioides* were somewhat different from all the other compressions. They had higher values of the 'A' factor and CH_2/CH_3, thereby showing similarities to some cutinite macerals and cuticles (Figs. 8 and 9), probably reflecting the contribution from a thick cuticle, for which this species is known (Zodrow, 2007). Compressions of all taxa were Type II kerogen, having medium 'A' factor values and the lowest 'C' factors, which could be interpreted as a relatively medium contribution from aliphatic groups and the lowest content of oxygen-containing compounds, respectively.

As the thermal histories of compressions, coal samples and coal macerals were similar, functional-group similarities among them are considered as additional support for our previous statements regarding compressions as being mini coal seams

Table 5
Semi-quantitative FTIR data relating to sample forms of gymnospermous pteridosperms of *Alethopteris pseudograndinioides*, *A. ambigua*, *Macroneuropteris scheuchzeri*, *Trigonocarpus grandis*; gymnospermous cordaitean of *Cordaites principalis* and associated coal (vitrain) samples. (Sydney Coalfield, Canada; Comp, compression; F. cuticle, fossilized cuticle.)

Sample	Taxon	Sample form	CH_2/CH_3	Al/Ox	C=O/C=C	C=O cont.	C=C cont.	Al/C=C	'A' factor	'C' factor
	Gymnospermous pteridosperms									
1	*Alethopteris pseudograndinioides*	Acid	1.2	0.10	0.027	0.022	0.81	0.13	0.11	0.026
2	*A. pseudograndinioides*	Alkaline	4.1	0.06	0.40	0.029	0.07	0.84	0.46	0.29
16	*Alethopteris ambigua*	Alkaline	3.3	0.14	0.10	0.054	0.53	0.26	0.21	0.092
15	*Macroneuropteris scheuchzeri*	Alkaline	3.2	0.20	0.39	0.054	0.14	1.43	0.59	0.28
14	*Trigonocarpus grandis*	Alkaline	3.8	0.16	0.26	0.037	0.14	1.08	0.52	0.20
3	*A. pseudograndinioides*	Comp	4.1	2.02	0.17	0.140	0.83	2.43	0.71	0.15
4	*A. pseudograndinioides*	Comp	5.6	0.84	0.80	0.340	0.42	2.0	0.67	0.44
5	*A. pseudograndinioides*	Comp	4.7	1.48	0.11	0.096	0.84	1.76	0.64	0.10
6	*A. pseudograndinioides*	Comp	5.1	1.16	0.29	0.230	0.77	1.50	0.60	0.23
7	*A. pseudograndinioides*	Comp	4.6	1.30	0.066	0.054	0.83	1.58	0.61	0.062
8	*A. pseudograndinioides*	Comp	3.2	1.05	0.36	0.270	0.73	1.43	0.59	0.27
26	*A. ambigua*	Comp	2.1	0.57	0.016	0.011	0.68	0.85	0.46	0.016
27	*A. ambigua*	Comp	1.7	0.59	0.032	0.027	0.84	0.70	0.41	0.031
28	*A. ambigua*	Comp	1.9	0.51	0.047	0.046	0.97	0.53	0.35	0.045
29	*A. ambigua*	Comp	2.2	0.55	0.020	0.014	0.70	0.78	0.44	0.020
30	*A. ambigua*	Comp	1.8	0.55	0.033	0.025	0.76	0.73	0.42	0.031
31	*A. ambigua*	Comp	2.5	0.59	0.035	0.028	0.81	0.73	0.42	0.034
32	*M. scheuchzeri*	Comp	3.5	0.71	0.015	0.007	0.48	1.48	0.60	0.015
33	*M. scheuchzeri*	Comp	2.5	0.55	0.015	0.009	0.60	0.93	0.48	0.015
34	*M. scheuchzeri*	Comp	2.3	0.58	0.016	0.009	0.60	0.98	0.49	0.015
35	*M. scheuchzeri*	Comp	3.3	0.59	0.015	0.008	0.52	1.14	0.53	0.015
36	*M. scheuchzeri*	Comp	3.3	0.58	0.016	0.008	0.51	1.14	0.53	0.016
37	*M. scheuchzeri*	Comp	2.4	0.62	0.025	0.013	0.55	1.14	0.53	0.024
38	*T. grandis*	Comp	0.9	0.48	0.001	0.001	0.94	0.51	0.34	0.001
39	*T. grandis*	Comp	0.9	0.45	0.002	0.002	0.92	0.49	0.33	0.002
40	*T. grandis*	Comp	0.9	0.52	0.001	0.001	0.93	0.56	0.36	0.001
41	*T. grandis*	Comp	0.9	0.43	0.003	0.003	0.92	0.47	0.32	0.003
42	*T. grandis*	Comp	1.2	0.58	0.001	0.001	0.94	0.62	0.38	0.001
23	*A. ambigua*	F. cuticle	5.6	1.01	0.38	0.039	0.10	9.98	0.91	0.28
24	*A. ambigua*	F. cuticle	4.8	0.96	0.18	0.022	0.13	7.65	0.88	0.15
25	*A. ambigua*	F. cuticle	5.7	0.87	0.44	0.053	0.12	7.18	0.88	0.31
43	*A. pseudograndinioides*	Cuticle	8.7	0.54	3.0	0.12	0.04	13.55	0.93	0.75
44	*A. pseudograndinioides*	Cuticle	7.6	0.65	7.1	0.40	0.06	11.62	0.92	0.88
45	*A. pseudograndinioides*	Cuticle	9.7	1.65	5.1	0.45	0.09	18.67	0.95	0.83
46	*A. pseudograndinioides*	Cuticle	9.6	1.75	4.0	0.32	0.08	21.38	0.96	0.80
47	*A. pseudograndinioides*	Cuticle	11.5	1.29	5.7	0.37	0.06	19.86	0.95	0.85
48	*A. ambigua-rachis*	Cuticle	10.6	0.34	1.3	0.08	0.06	5.61	0.85	0.56
49	*A. ambigua*	Cuticle	4.1	0.38	0.21	0.03	0.13	2.91	0.74	0.18
50	*A. ambigua*	Cuticle	4.6	0.36	0.39	0.04	0.10	3.66	0.79	0.28
51	*A. ambigua*	Cuticle	3.8	0.38	0.39	0.04	0.10	3.61	0.78	0.28
52	*A. ambigua*	Cuticle	5.0	0.42	0.69	0.05	0.07	6.29	0.86	0.41
53	*A. ambigua*	Cuticle	5.0	0.39	0.25	0.03	0.12	3.14	0.76	0.20
54	*A. ambigua*	Cuticle	5.1	0.40	1.4	0.08	0.05	7.45	0.88	0.59
55	*M. scheuchzeri*	Cuticle	1.2	0.63	4.8	0.26	0.05	11.82	0.92	0.83
60	*T. grandis*	Cuticle	VH[a]	0.59	6.2	0.35	0.06	10.45	0.91	0.86
61	*T. grandis*	Cuticle	18.5	0.78	2.4	0.09	0.04	20.87	0.95	0.71
62	*T. grandis*	Cuticle	VH[a]	0.64	1.7	0.06	0.04	16.61	0.94	0.62
	Gymnospermous cordaitean									
13	*Cordaites principalis*	Alkaline	2.9	0.13	0.099	0.016	0.16	0.85	0.46	0.09
9	*C. principalis*	Comp	2.4	0.52	0.010	0.009	0.84	0.62	0.38	0.01
10	*C. principalis*	Comp	2.0	0.54	0.008	0.006	0.76	0.72	0.42	0.008
11	*C. principalis*	Comp	2.3	0.59	0.005	0.004	0.77	0.76	0.43	0.005
12	*C. principalis*	Comp	2.3	0.62	0.004	0.003	0.79	0.78	0.44	0.004
56	*C. principalis*	Cuticle	1.1	0.45	2.4	0.30	0.13	3.53	0.78	0.70
57	*C. principalis*	Cuticle	1.1	0.34	3.3	0.32	0.10	3.43	0.77	0.77
58	*C. principalis*	Cuticle	1.1	0.41	2.4	0.32	0.13	3.16	0.76	0.71
59	*C. principalis*	Cuticle	1.1	0.41	2.4	0.31	0.13	3.22	0.76	0.71
	Coal (vitrain) Sydney									
17	6-mm band	Vitrain	0.9	0.54	0.003	0.002	0.77	0.69	0.41	0.003
18	5-mm band	Vitrain	0.8	0.74	0.004	0.004	1.09	0.69	0.41	0.004
19	3-mm band	Vitrain	0.8	0.40	0.026	0.020	0.74	0.54	0.35	0.026
21	2-mm band	Vitrain	0.8	0.69	0.001	0.001	1.07	0.65	0.39	0.001
22	5-mm band	Vitrain	0.8	0.62	0.001	0.001	1.07	0.58	0.37	0.001
20	Mixture fusinite + vitrain	V + F[b]	1.0	0.42	0.007	0.005	0.64	0.67	0.40	0.007

[a] Very high values of CH_2/CH_3: the contribution of antisymmetric and symmetric C—H stretching vibrations of CH_3 groups is nearly zero.
[b] Mixture, fusinite + vitrain + pyrite.

(Zodrow et al., 2009) with a composition similar to that of some coals and coal macerals (i.e. resinites, sporinites and vitrinites).

4.2.6. Summary

By way of concluding the comparison among the different sample forms and coal macerals, the following observations are

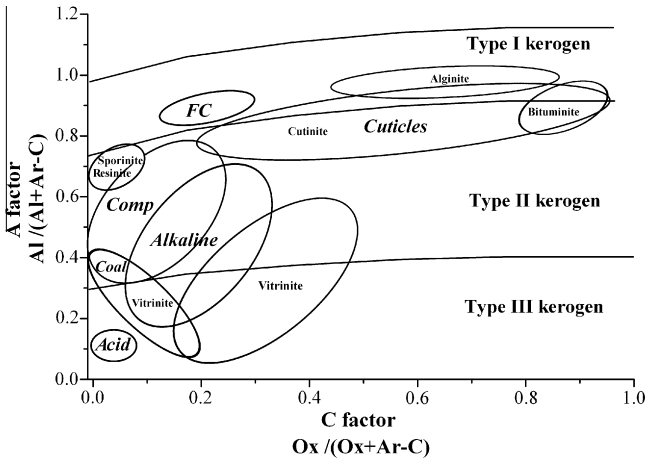

Fig. 9. Simplified plot of Fig. 8 indicating approximate regions of different sample forms (ellipses around the groups do not have any statistical significance).

offered. Cuticles, coals, compressions and the corresponding alkaline solutions of some of the taxa showed a composition similar to that of Type II kerogen. The exceptions were the cuticles of *A. pseudograndinioides* and *T. grandis* (Type I kerogen) and the alkaline solution of *A. ambigua* (Type III kerogen). The acidic solution (of *A. pseudograndinioides*) was similar in composition to Type III kerogen, while fossilized cuticles were Type I kerogen (Figs. 8 and 9). The cuticles were similar to some alginites, bituminites and cutinites; compressions showed similarities to some resinites, sporinites and cutinites, while coals and alkaline and acidic solutions were mainly similar to some vitrinites (Figs. 8 and 9). Fossilized cuticles were different from all the coal macerals considered, as their diagenetic history is considered different, though not yet fully understood.

Regarding 'A' and 'C' factors, a transitional change in the contents of aliphatic and oxygen-containing compounds from cuticles to alkaline solutions to compressions is evident. Thus, high values of aliphatic and oxygen-containing compounds occurred for cuticles, with intermediate values for fossilized cuticles and alkaline solutions, while mainly aromatic compounds with a relatively poor oxygen content characterized compressions, acidic solution and coals (Figs. 8 and 9). For all the taxa, and considering the CH_2/CH_3 ratio, cuticles showed the highest values, whereas medium values were found for alkaline solutions and fossilized cuticles. Acidic solutions, compressions and coal exhibited the lowest ratio values of the same variable (Table 5).

Among the entire set of sample forms, remarkable similarities (regarding 'A' and 'C' factors and CH_2/CH_3 ratio) were found between cuticles of *T. grandis* ovules and *A. pseudograndinioides* leaves. Since these plant organs are found in physical association with one another (Zodrow, 2007), FTIR-derived data are suggestive of the likely application of the technique to whole-plant reconstruction, given conditions that include similar or the same diagenetic conditions of plant organs physically associated at more than one stratigraphic locality. However, there are problems by way of non-existing nomenclature rules for naming whole fossil plants (see Pšenička and Zodrow, 2010). Cleal and Zodrow (2010) discussed the specific case involving the *T. grandis* ovule.

4.3. PCA

The larger number of data points (496: 62 samples and eight attributes, Table 5) provided an opportunity for PCA to focus on grouping data as a function of chemical structure or functional groups, given the six sample forms and the chemical data. This is termed PCA[A]. We performed a second analysis, PCA[B], using only the 33 compression and six Sydney coal (vitrain) samples, restricting them to four attributes, viz. CH_2/CH_3, 'A' factor, C=O/C=C and C=C cont. (aromatic carbon contribution). This approach, by eliminating some sample forms attributed as redundant, clearly focuses on mapping out a chemotaxonomic potential for future study.

4.3.1. PCA[A] of compressions, cuticles, fossilized cuticles, Schulze's solutions and coal samples

Cumulatively, two components accounted for 80.09% of the variance; the loading plots and scores are shown in Figs. 10 and 11, respectively. The most important component (65.9% of the explained variance) involved mainly negative loadings, except for the moderate positive loading on C=C cont., which emphasized the abundance of aromatic carbon groups vs. the other functional groups. Cuticles of *A. pseudograndinioides* and *T. grandis* exhibited the most negative scores (Fig. 11, *x* axis), reflecting their low content of aromatic carbon groups. This was clearly shown by the lowest C=C cont. values and the high values of both Al/C=C and 'C' factor. In general terms, the remaining cuticles (taxa) exhibited the same trends.

The second component (14.2% of variance accounted for) was negative. The majority of cuticles and all the Schulze's solutions showed positive scores against this component (Fig. 11, *y* axis), as a result of the Al/Ox values being among the lowest in the entire sample set (Table 5).

The plot of scores (Fig. 11) was particularly useful in showing the different grouping of data as a function of chemical structure (functional groups), and in reflecting the nature of the six sample forms. Fig. 12 is a simplified plot where the groupings of the six sample forms are indicated by delimiting ellipses around these groups (for clarity only).

Though small in number of samples, the group representing fossilized cuticles of *A. ambigua* was well separated from the other groups, having an intermediate position between compressions and cuticles. More importantly, fossilized cuticles were separated from compressions, as hypothesized in previous studies (Zodrow and Mastalerz, 2009; Zodrow et al., 2009). Regarding cuticles, the plot of scores (Fig. 11) was especially effective in revealing groupings for *A. pseudograndinioides*, *T. grandis*, *M. scheuchzeri* and *C. principalis*. These groupings coincide with a taxonomic classification based on morphological characters, noting no overlapping of samples (morphotaxa).

In Fig. 11, cuticles of *C. principalis* and *A. ambigua* form a tight group on the scores plot. Cuticles of *A. pseudograndinioides* (leaf) and of *T. grandis* (physically associated ovule) formed a group,

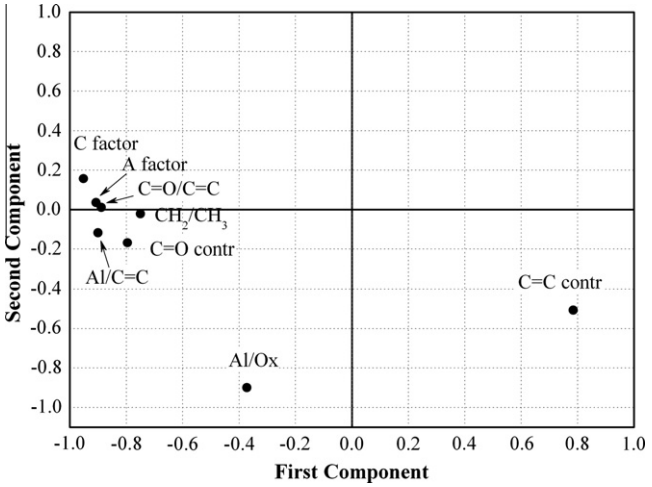

Fig. 10. PCA[A]: plot of component loadings.

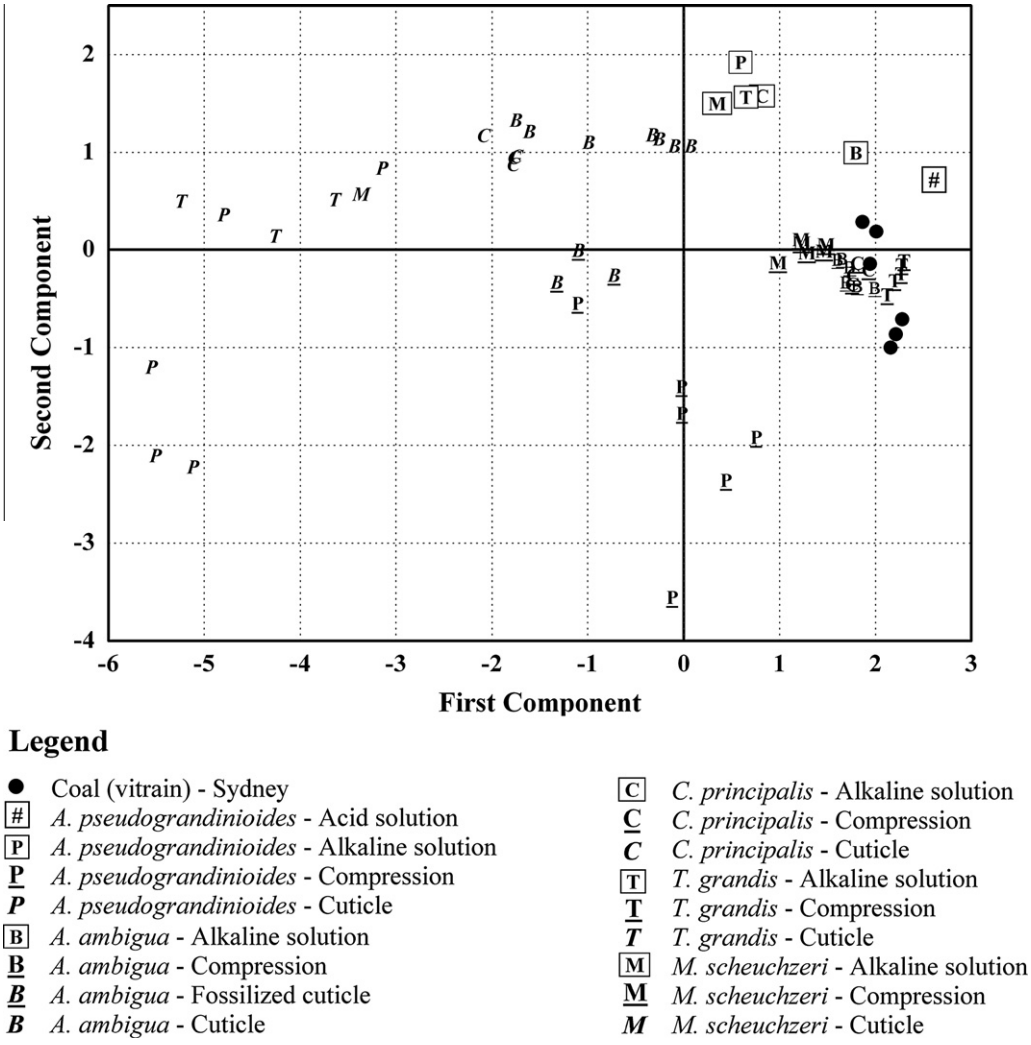

Fig. 11. PCA[A]: plot of component scores. See text for explanation of PCA[A].

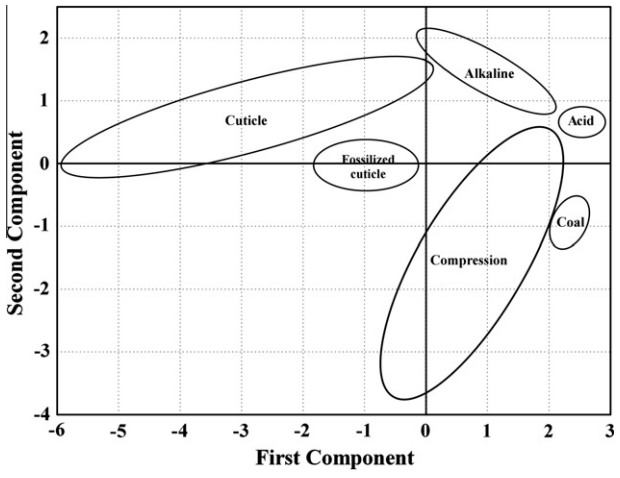

Fig. 12. Simplified plot showing groupings of fossil-derived data as indicated by approximate delimited elliptical zones that do not have any statistical significance.

being well separated from the other fossil forms. Interestingly, this grouping supports studies which suggest a chemical link between these two taxa, which are frequently found in physical association (Cleal and Zodrow, 2010).

In contrast, compressions and coals formed a tight group (the exception being the compressions assigned to *A. pseudograndinioides*, Fig. 11). In order to find a further distinction between the samples of this tight group, PCA[B] was performed (Section 4.3.2). Compressions assigned to *A. pseudograndinioides* showed the most negative scores on the second component (Fig. 11) which could be associated with extreme values for two variables: Al/Ox and C=C cont. Mean values calculated (not shown) for these variables of compressed *A. pseudograndinioides* were 1.31 and 0.74, respectively. This was compared with mean values across all 62 samples of 0.63 (Al/Ox) and 0.47 (C=C cont.). Such a result could be interpreted as having chemotaxonomic value, i.e. the scores (Fig. 11) discriminate between samples of compressions of *A. pseudograndinioides* on the basis of functional groups.

4.3.2. PCA[B] of compressions and coal samples

A two-component solution (87.3% of explained variance) was acceptable, assuming that in the face of the sharp drop in eigenvalues from 2.83 to 0.66, the second component was still an estimator of the population component and not merely a mathematical construct (Kendall, 1965). Fig. 13 shows the loading plot and Fig. 14 the component scores. The first component (70.7%) showed positive loadings on CH_2/CH_3, 'A' factor and C=O/C=C, and a negative loading on C=C cont. This component reflects the abundance of aliphatic and oxygen-containing functional groups.

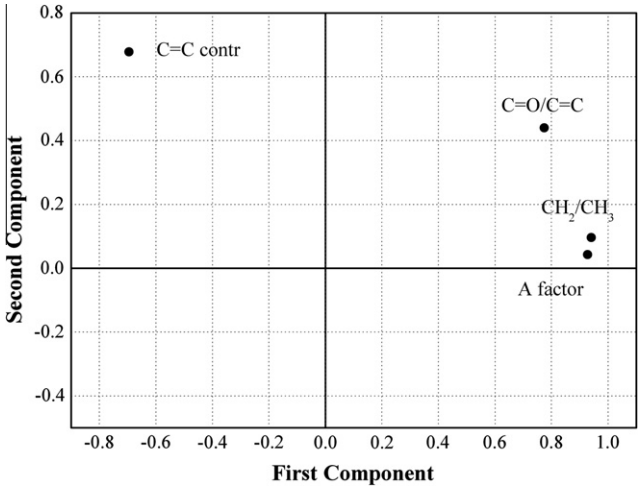

Fig. 13. PCA[B]: plot of component loadings.

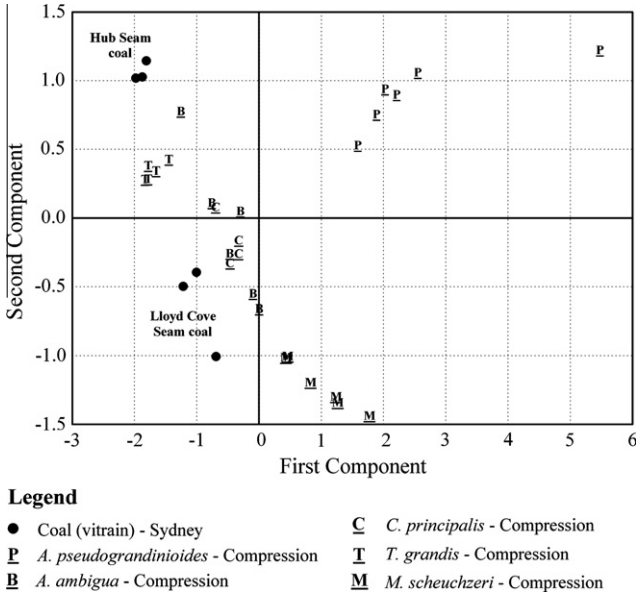

Fig. 14. PCA[B]: plot of component scores. See text for explanation of PCA[B].

Compressions of *A. pseudograndinioides* samples separated well from the other compressions and coal and exhibited the most positive scores (Fig. 14, *x* axis), reflecting the high content of aliphatic and oxygen-containing groups. This is clearly shown by the high values of CH_2/CH_3, 'A' factor and C=O/C=C ratio recorded for *A. pseudograndinioides* compressions.

The second component (16.5%) showed a very high positive loading on C=C cont. and a moderate positive loading on C=O/C=C ratio (Fig. 13), likely reflecting the abundance of aromatic carbon functional groups. Coals (from the Hub Seam) and compressions of *T. grandis* exhibited the most positive scores (Fig. 14, *y* axis), reflecting the high content of aromatic carbon groups. At the other extreme, *M. scheuchzeri* compressions separated well and exhibited the most negative scores (Fig. 14, *y* axis) as a result of the C=C cont. ratio being among the lowest in the entire sample set (Table 5).

It is clear from the scores (Fig. 14) that three out of five compression-preserved taxa were distinctly separated by PCA[B], namely *A. pseudograndinioides*, *T. grandis*, and *M. scheuchzeri*. The results are interpreted as revealing differences which are of chemosystematic significance. In contrast, compressions of *C. principalis* and *A. ambigua* were not clearly separated (Fig. 14), which is probably based on their similar chemical compositions.

The coal samples (Fig. 14, *y* axis) formed two different groups, indicating clear differences regarding their aromatic, aliphatic and oxygen-containing functional groups, which is probably related to incrementally increased maturity. One group (all three from the Hub Seam) plotted closely together, revealing a similar composition. The other three (Lloyd Cove Seam) formed a different group, based on a comparatively more aliphatic composition. Two were well separated from the third sample, made up of a mixture of macerals (fusinite + vitrain). The results indicate that samples from the Hub Seam samples have a higher content of aromatic compounds than Lloyd Cove Seam samples. The latter are characterized by a higher content of oxygen-containing functional groups (higher values of C=O/C=C; Table 5).

The results of the PC analyses reinforce our previous observation on the compressions, coals and coal macerals that a compression is similar to being a mini coal seam (Zodrow et al., 2009). From Figs. 8 and 9 (kerogen type diagrams using only two IR variables), it is evident that compressions and coals share similar functional groups. Furthermore, Figs. 11 and 12 (PCA[A]), clearly demonstrate the similarities between compressions and coals as revealed from the analysis of all the available FTIR variables. Finally, Fig. 14 (PCA[B]) leaves little doubt about the use of certain FTIR-derived variables (CH_2/CH_3, C=O/C=C, C=C cont. and 'A' factor) for discriminating coal samples and different fossil taxa. It is important to observe that groupings coincide with taxonomic classification (based on morphology), with no overlapping of samples (morphotaxa). This could be interpreted as their having a similar biochemical origin, as the thermal histories of the compressions are the same, i.e. there is a possibility of preservation of compounds (or molecular fragments) in compressions, synthesized by the original plants.

5. Conclusions

We used FTIR spectroscopy analysis for the study of functional groups for characterizing a number of organic moieties in Pennsylvanian-age gymnosperm foliage, viz., medullosalean and cordaitean foliage, and additionally in coal samples of the same age from two coalfields in Maritime Canada. Specifically, five sample forms resulted from combining different plant fossil preservation with sample chemical preparation by using Schulze's process. The resultant FTIR data were organized into a data matrix with eight variables and 62 samples, which reduced to a two principal component model with 80% cumulative variance. Guided by this model, a four-variable data matrix was devised, from which two components were extracted (87% cumulative variance) which focused on the coaly preservation (compression and Sydney vitrain coal samples). The desired result of being able to better focus on groupings as a function of functional group (=multivariate model) was achieved the following conclusive points being emphasized:

(i) Overall, the multivariate model supports Pennsylvanian fossil-leaf chemotaxonomy (which we have assumed via working hypothesis since 1992).
(ii) Support was additionally garnered, with caveats, for the evolving science of Carboniferous whole-plant reconstruction, especially using spectrochemical methodology in combination with classical compression–cuticle morphologies to build credible models from physically associated plant organs.
(iii) Not negated is the hypothesis of no difference between a compression fossil and its associate coal seam, provided thermal integrity is maintained within the stratum section of the coal seam and its roof rocks.

(iv) Some common chemical characteristics exist between kerogen Types I and II and our data.
(v) We suggest that Schulze's process mimics the natural processes taking part in aspects of kerogen formation and hypothesize that at the basis of kerogen genesis Eh-pH phase diagrams matter.

Acknowledgements

We thank D. Keefe, Department of Chemistry, Molecular Spectroscopy Research Laboratory and M. Jones, Department of Biology, Cape Breton University, for the use of an IR instrument and Nomarski phase-contrast microscope, respectively. We also thank N. Sherwood and C. Marshall for time and effort in improving the manuscript. Partial financial support from Universidad Nacional de Cuyo (SeCTyP, Project 06/M012) is gratefully acknowledged.

Appendix A. Supplementary material

Supplementary data associated with this article can be found, in the online version, at doi:10.1016/j.orggeochem.2010.09.010.

Associate Editor—**S.C. George**

References

Almendros, G., Sanz, J., 1992. A structural study of alkyl polymers in soil after perborate degradation of humin. Geoderma 53, 79–95.
Almendros, G., Dorado, J., Sanz, J., Alvarez-Ramis, C., Fernández-Marrón, M.T., Archangelsky, S., 1999. Compounds released by sequential chemolysis from cuticular remains of the Cretaceous Gymnosperm *Squamastrobus tigrensis* (Patagonia, the Argentine). Organic Geochemistry 30, 623–634.
Anderson, T.W., 2003. An Introduction to Multivariate Statistical Analysis (Wiley Series in Probability and Statistics), third ed. John Wiley & Sons. 752 pp.
Cleal, C.J., Zodrow, E.L., 1989. Epidermal structure of some medullosan *Neuropteris* foliage from the Middle and Upper Carboniferous of Canada and Germany. Paleontology 32, 837–882.
Cleal, C.J., Zodrow, E.L., 2010. An association of *Alethopteris* foliage, *Trigonocarpus* ovules and *Bernaultia*-like pollen organs from the Middle Pennsylvanian of Nova Scotia. Palaeontographica Abteilung B 283, 73–97.
Cleal, C.J., Shute, C.H., Zodrow, E.L., 1990. A revised taxonomy for Palaeozoic neuropterid foliage. Taxon 39, 486–492.
Colthup, N.B., Daly, L.H., Wiberley, S.E., 1990. Introduction to Infrared and Raman Spectroscopy. Academic Press, New York. 547 pp.
D'Angelo, J.A., 2004. FT-IR determination of aliphatic and aromatic C—H contents of fossil leaf compressions. Part 2: applications. Anuario Latinoamericano de Educación Química (ALDEQ) 18, 34–38.
D'Angelo, J.A., 2006. Analysis by Fourier transform infrared spectroscopy of *Johnstonia* (Corystospermales, Corystospermaceae) cuticles and compressions from the Triassic of Cacheuta, Mendoza, Argentina. Ameghiniana 43, 669–685.
D'Angelo, J.A., Marchevsky, E., 2004. FT-IR determination of aliphatic and aromatic C—H contents of fossil leaf compressions. Part 1: analysis, curve-resolving and choice of bands. Anuario Latinoamericano de Educación Química (ALDEQ) 17, 37–41.
Dimitrova, T.K., Zodrow, E.L., Cleal, C.J., Thomas, B.A., in press. Palynological evidence for Pennsylvanian (Late Carboniferous) vegetation changes in the Sydney Coalfield, Eastern Canada. Geological Magazine.
Durig, D.T., Esterle, J.S., Dickson, T.J., Durig, J.R., 1988. An investigation of the chemical variability of woody peat by FT-IR Spectroscopy. Applied Spectroscopy 42, 1239–1244.
Ganz, H., Kalkreuth, W., 1987. Application of infrared spectroscopy to the classification of kerogen-types and the evolution of source rock and oil–shale potentials. Fuel 66, 708–711.
Gauglitz, G., Vo-Dinh, T., 2003. Handbook of Spectroscopy. WILEY-VCH Verlag GmbH & Co. KGaA, Weinheim. 538 pp.
Guo, Y., Bustin, R.M., 1998. Micro-FTIR spectroscopy of liptinite macerals in coal. International Journal of Coal Geology 36, 259–275.
Izenman, A.J., 2008. Modern Multivariate Statistical Techniques: Regression, Classification, and Manifold Learning (Springer Texts in Statistics), first ed. Springer. 734 pp.
Johnson, R.A., Wichern, D.W., 2008. Applied Multivariate Statistical Analysis, sixth ed. Pearson Education Limited. 761 pp.
Jolliffe, I.T., 2002. Principal Component Analysis, second ed. Springer. 487 pp.
Kaiser, H.F., 1960. The application of electronic computers to factor analysis. Educational and Psychological Measurement 20, 141–151.
Kauppinen, J.K., Moffatt, D.J., Mantsch, H.H., Cameron, D.G., 1981a. Fourier transform in the computation of self-deconvoluted and first order derivative spectra of overlapped band contours. Analytical Chemistry 53, 1454–1457.
Kauppinen, J.K., Moffatt, D.J., Mantsch, H.H., Cameron, D.G., 1981b. Fourier self-deconvolution: a method for resolved intrinsically overlapped bands. Applied Spectroscopy 35, 271–276.
Kendall, M.G., 1965. A Course in Multivariate Analysis. Third Impression. Charles Griffin & C. Ltd., London. 185 pp.
Lattin, J., Carroll, D., Green, P., 2002. Analyzing Multivariate Data (Duxbury Applied Series), first ed. Duxbury Press. 560 pp.
Lin, R., Ritz, G.P., 1993a. Reflectance FT-IR microspectroscopy of fossil algae contained in organic-rich shale. Applied Spectroscopy 47, 265–271.
Lin, R., Ritz, G.P., 1993b. Studying individual macerals using i.r. microspectroscopy, and implications on oil versus gas/condensate proneness and "low-rank" generation. Organic Geochemistry 20, 695–706.
Lyons, P.C., Zodrow, E.L., Orem, W.H., 1992. Coalification of cuticles and compressed leaf tissue of the Carboniferous seed fern *Macroneuropteris* (*Neuropteris*) *scheuchzeri* – implication to the bituminous coal stage. In: Annual Meeting, Abstract with Programs, Cincinnati, Ohio, USA, October 1992. Geological Society of America, 1992, p. A163
Lyons, P.C., Orem, W.H., Mastalerz, M., Zodrow, E.L., Vieth-Redemann, A., Bustin, R.M., 1995. ^{13}C NMR, micro-FTIR and fluorescence spectra, and pyrolysis-gas chromatograms of coalified foliage of late Carboniferous medullosan seed ferns, Nova Scotia, Canada: implications for coalification and chemotaxonomy. International Journal of Coal Geology 27, 227–248.
Lyons, P.C., Zodrow, E.L., Millay, M.A., Dolby, G., Gillis, K.S., Cross, A.T., 1997. Coal-ball floras of Maritime Canada and palynology of the Foord seam: geologic, paleobotanical and paleoecological implications. Review of Palaeobotany and Palynology 95, 31–50.
Mastalerz, M., Bustin, R.M., 1993. Electron microprobe and micro-FTIR analyses applied to maceral chemistry. International Journal of Coal Geology 24, 333–345.
Mastalerz, M., Bustin, R.M., 1996. Application of reflectance micro-Fourier Transform infrared analysis to the study of coal macerals: an example from the Late Jurassic to Early Cretaceous coals of the Mist Mountain Formation, British Columbia, Canada. International Journal of Coal Geology 32, 55–67.
Painter, P.C., Coleman, M.M., Snyder, R.W., Mahajan, O., Komatsu, M., Walker Jr., P.L., 1981a. Low temperature air oxidation of coking coals: Fourier transform infrared studies. Applied Spectroscopy 35, 106–110.
Painter, P.C., Snyder, R.W., Starsinic, M., Coleman, M.M., Kuehn, D.W., Davis, A., 1981b. Concerning the application of FT-infrared to the study of coal: a critical assessment of band assignments and the application of spectral analysis programs. Applied Spectroscopy 35, 475–485.
Painter, P.C., Starsinic, M., Coleman, M.M., 1985. Determination of functional groups in coal by Fourier transform interferometry. In: Ferraro, J.R., Basile, L.J. (Eds.), Fourier Transform Infrared Spectroscopy, vol. 4. Academic Press, New York, pp. 169–240.
Pšenička, J., Zodrow, E.L., 2010. Reconstruction of extinct plants: tyranny of nomenclature and spectrochemistry. In: 8th European Palaeobotany-Palynology Conference 2010, 6–10 July 2010, Budapest, Hungary. Program and Abstracts, p. 185.
Rencher, A.C., 2002. Methods of Multivariate Analysis (Wiley Series in Probability and Statistics Series), vol. 1, second ed. John Wiley & Sons. 738 pp.
Rosenfeld, A., Kak, A.C., 1982. Digital Picture Processing, vol. 1, second ed. Academic Press, New York, p. 35 pp.
Schulze, F., 1855. Bemerkungen über das Vorkommen wohlerhaltener Cellulose in Braunkohle und Steinkohle. Bericht Verhandlungen königlich-preussischen Akademie der Wissenschaften, Berlin. pp. 676–678.
Shurvell, H.F., 2002. Spectra–structure correlations in the mid- and far-infrared. In: Chalmers, J., Griffiths, P. (Eds.), Handbook of Vibrational Spectroscopy, Sample Characterization and Spectral Data Processing, vol. 3. John Wiley & Sons Ltd., Chichester. 11 pp.
Shute, C.H., Cleal, C.J., 1987. Palaeobotany in museums. Geological Curator 4, 553–559.
Smith, B.C., 1996. Fundamentals of Fourier Transform Infrared Spectroscopy. CRC Press, London. pp. 202.
Sobkowiak, M., Painter, P., 1992. Determination of the aliphatic and aromatic CH contents of coals by FT-i.r.: studies of coal extracts. Fuel 71, 1105–1125.
StatSoft Inc., 2001. STATISTICA (Data Analysis Software system), Version 6. <www.statsoft.com>.
Stuart, B., 2004. Infrared Spectroscopy: Fundamentals and Applications. John Wiley & Sons Ltd., England. 224 pp.
Taylor, T.N., Taylor, E.L., 1993. The Biology and Evolution of Fossil Plants. Prentice-Hall, Englewood Cliffs, NJ. 982 pp.
Wang, S.H., Griffiths, P.R., 1985. Resolution enhancement of diffuse reflectance i.r. spectra of coals by Fourier self-deconvolution. 1. C—H stretching and bending modes. Fuel 64, 229–236.
Zodrow, E.L., 2007. Reconstructed tree fern *Alethopteris zeilleri* (Carboniferous, Medullosales). International Journal of Coal Geology 69, 68–89.
Zodrow, E.L., Cleal, C.J., 1998. Revision of the pteridosperm foliage *Alethopteris* and *Lonchopteridium* (Upper Carboniferous), Sydney Coalfielf, Nova Scotia, Canada. Palaeontographica Abteilung B. 247, 65–122.
Zodrow, E.L., Mastalerz, M., 2001. Chemotaxonomy for naturally macerated tree-fern cuticles (Medullosales and Marattiales), Carboniferous Sydney and Mabou Sub-Basins, Nova Scotia, Canada. International Journal of Coal Geology 47, 255–275.
Zodrow, E.L., Mastalerz, M., 2002. FTIR and py-GC–MS spectra of true-fern and seed-fern sphenopterids (Sydney Coalfield, Nova Scotia, Canada, Pennsylvanian). International Journal of Coal Geology 51, 111–127.

Zodrow, E.L., Mastalerz, M., 2007. Functional groups in a single pteridosperm species: variability and circumscription (Pennsylvanian, Nova Scotia, Canada). International Journal of Coal Geology 70, 313–324.

Zodrow, E.L., Mastalerz, M., 2009. A proposed origin for fossilized Pennsylvanian plant cuticles by pyrite oxidation (Sydney Coalfield, Nova Scotia, Canada). Bulletin of Geosciences 84, 227–240.

Zodrow, E.L., Mastalerz, M., Orem, W.H., Šimůnek, Z., Bashforth, A.R., 2000a. Functional groups and elemental analyses of cuticular morphotypes of Cordaites principalis (Germar) Geinitz, Carboniferous Maritimes Basin, Canada. International Journal of Coal Geology 45, 1–19.

Zodrow, E.L., Šimůnek, Z., Bashforth, A.R., 2000b. New cuticular morphotypes of *Cordaites principalis* from the Canadian Carboniferous Maritimes Basin. Canadian Journal of Botany 78, 135–148.

Zodrow, E.L., D'Angelo, J.A., Mastalerz, M., Keefe, D., 2009. Compression-cuticle of seed ferns: insights from liquid–solid states FTIR (Late Palaeozoic-Early Mesozoic, Canada–Spain–Argentina). International Journal of Coal Geology 79, 61–73.